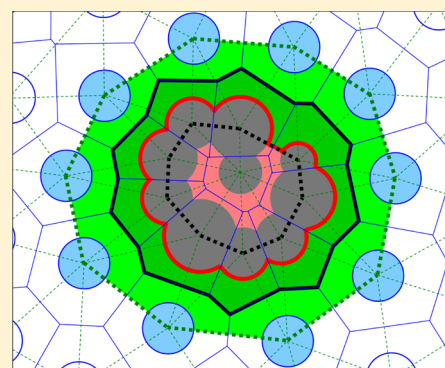


Disentangling Volumetric and Hydrational Properties of Proteins

Vladimir P. Voloshin,[†] Nikolai N. Medvedev,^{†,‡} Nikolai Smolin,[§] Alfons Geiger,^{||} and Roland Winter^{*,||}[†]Institute of Chemical Kinetics and Combustion, SB RAS, 630090 Novosibirsk, Russia[‡]Novosibirsk State University, 630090 Novosibirsk, Russia[§]Department of Cell and Molecular Physiology, Stritch School of Medicine, Loyola University Chicago, Maywood, Illinois 60153, United States^{||}Physikalische Chemie, Fakultät für Chemie und Chemische Biologie, Technische Universität Dortmund, Otto-Hahn-Strasse 6, 44221 Dortmund, Germany

ABSTRACT: We used molecular dynamics simulations of a typical monomeric protein, SNase, in combination with Voronoi–Delaunay tessellation to study and analyze the temperature dependence of the apparent volume, V_{app} , of the solute. We show that the void volume, V_{B} , created in the boundary region between solute and solvent, determines the temperature dependence of V_{app} to a major extent. The less pronounced but still significant temperature dependence of the molecular volume of the solute, V_{M} , is essentially the result of the expansivity of its internal voids, as the van der Waals contribution to V_{M} is practically independent of temperature. Results for polypeptides of different chemical nature feature a similar temperature behavior, suggesting that the boundary/hydration contribution seems to be a universal part of the temperature dependence of V_{app} . The results presented here shine new light on the discussion surrounding the physical basis for understanding and decomposing the volumetric properties of proteins and biomolecules in general.



■ INTRODUCTION

The physical–chemical properties of proteins control their function and as such have been the object of intense investigations for many decades now.^{1–3} Progress in the understanding of protein structure, thermodynamics, dynamics, and hence function has been made thanks to major advances in experimental and computational approaches in recent years. Despite this progress, a complete description of the factors that control these properties has not been achieved. On the one hand, the characterization of the role of the solvent in controlling protein conformational transitions and stability remains to be accomplished.³ On the other hand, insight into temperature effects and understanding of the temperature–pressure stability diagram of proteins has lagged behind.^{4–14} The latter requires a profound understanding of the molecular contributions to the value of the volume change upon unfolding which has remained elusive but is also of fundamental interest for optimizing biotechnological processes, such as in the field of baroenzymology.^{8,9,11}

The change in the apparent volume, V_{app} (or partial molar volume at infinite dilution), upon unfolding of a protein, $V_{\text{app}}^{\text{unf}} - V_{\text{app}}^{\text{native}}$, is generally thought to be due to the loss of internal void volume and the increase in hydrophilic hydration of more charged and polar groups. The method of dissecting this volume change, and hence V_{app} , into different contributions and their magnitudes are still a matter of debate, however.⁷

Generally, the volume of a protein is broken down into a number of different contributions. For example, following

Chalikian,^{15,16} the partial molar or apparent volume of a protein may be dissected into (1) the intrinsic volume, V_{int} , which originates from the protein molecule itself, (2) the thermal volume, V_{T} , which results from thermally induced mutual molecular vibrations and reorientations of the solute and the solvent at their interface, and (3) the interaction volume, V_{I} , describing—with regard to the bulk solvent—the solvent volume change associated with the hydration of solvent-accessible protein groups, resulting from solute–solvent interactions around the charged (electrostriction), polar (hydrogen-bonding), and nonpolar (hydrophobic hydration) atomic groups on the protein surface:¹⁵

$$V_{\text{app}} = V_{\text{int}} + V_{\text{T}} + V_{\text{I}} \quad (1)$$

(We do not include the term $k_{\text{B}}\beta_{\text{T}}T$, which takes into account translational degrees of freedom of the solute molecule, because it is negligible in our case.) The temperature and pressure derivatives of V_{app} , i.e., the coefficients of thermal expansion and compressibility of the protein, are thought to consist of similar contributions.

As discussed in ref 15, there are two conventional definitions of the intrinsic volume, V_{int} of a solute: it can be characterized by the Voronoi volume, V_{Vor} , of the molecule in solution, while the second definition uses the molecular volume, V_{M} , which

Received: October 30, 2014

Revised: December 22, 2014

Published: January 15, 2015

consists of the van der Waals volume of the constituent atoms including the volume of internal voids. The molecular volume is always smaller than the Voronoi volume because the latter includes a part of empty space of the protein–solvent boundary region. If one uses the molecular volume as intrinsic volume, this additional empty-space volume has to be assigned to the thermal volume as suggested by Chalikian et al.¹⁶

Please note that the dissection of the apparent volume into the additive terms shown in eq 1 is descriptive and probably approximate. In particular, the interplay between protein and water influences both V_T and V_I . By analysis of molecular dynamics models of protein solutions, it is impossible to dissect these contributions geometrically. A more simple dissection was used in refs 17 and 18:

$$V_{\text{app}} = V_{\text{int}} + \Delta V \quad (2)$$

Here, V_{int} is the intrinsic volume assigned to the protein, and ΔV is the contribution of the solvent, calculated as difference between the volume of the hydration shell and the volume of the same amount of water molecules (N_{hydr}) in bulk water, i.e., $\Delta V = V_{\text{hyd}} - N_{\text{hydr}}/\rho_0$ (ρ_0 is the number density of bulk water at the same temperature). However, in this approach, one has to define explicitly the border between protein and water as well as the extension of the hydration region. It turns out that the result is very sensitive to the definition of this interface and may lead to erroneous results.¹⁹

In our recent works,²⁰ we developed a technique for a quantitative analysis of volumetric characteristics, using molecular dynamics models of solutions. It is based on the Voronoi–Delaunay method, which provides a strict way for the separation of voids related to the solute molecule, the solvent, and their boundary region, thereby allowing to calculate both the apparent volume, V_{app} , and its components. We dissect V_{app} into the intrinsic volume (defined as the Voronoi volume here, i.e. $V_{\text{int}} = V_{\text{vor}}$; see below) and the hydration contribution ΔV as defined in eq 2. Moreover, we can dissect the intrinsic volume into the van der Waals volume of the protein, its internal voids, and its boundary void contribution. Besides, we can independently calculate the void volume between protein and solvent, V_B , which, in turn, can be divided into the voids belonging to the protein and solvent.

In this study, we set out to describe the contributions to the measured volumetric properties of a well-characterized monomeric protein, staphylococcal nuclease (SNase), and their complete temperature dependence, i.e., the expansivity, using results from molecular dynamics (MD) simulations, and we discuss the results also in the context of some previous results obtained for a natively unfolded peptide, the human islet amyloid polypeptide (hIAPP). The theoretical data obtained are then compared with experimental data as determined by pressure perturbation calorimetry (PPC). The volumetric properties are resolved into their various structural, interfacial, and hydrational contributions, aiming at shining new light on the longstanding debate surrounding the physical basis for understanding and decomposing the volumetric properties of proteins.

METHODS

In this paper we analyze new molecular dynamics simulations of an aqueous solution of staphylococcal nuclease (SNase). We performed molecular dynamics simulations using crystallographic heavy atoms coordinates obtained from the Protein

Data Bank (PDB), entry 1STN. Residues 1–6 and 142–149 were missing in the crystal structure. The starting structure of the protein for the simulation was completed by adding coordinates for residues 1–6 (taken from PDB entry 2SNS) and constructing residues 142–149 using modeling tools. Water molecules were identified crystallographically in 1STN and were included in the starting configuration. MD simulations were performed using the program GRO-MACS^{21,22} with the OPLS force field and SPC/E water model. For the residues we choose the protonation states corresponding to pH 7.0. The total charge of +8e on the protein was then neutralized by a uniform distribution of the opposite charge between all atoms in order to make the system neutral. This approach avoids the presence of ions which can disturb the structure of the water.²³ Energy minimization was performed on these initial structures, using the steepest descent method for 1000 steps, which were then solvated in a rectangular water box with a minimum of 10 Å from the surface of the protein to a face of the model box. Thus, the SNase molecule was surrounded by 10 907 water molecules. The particle mesh Ewald method was used to calculate the electrostatic interactions, and a cutoff of 9 Å was used for the short-range van der Waals interactions. Molecular dynamics simulations were carried out with an integration time step of 2 fs. To reach the target temperature, the Berendsen method was used. After 1 ns equilibration, production simulations were performed in the NPT ensemble using the Nosé–Hoover thermostat and a Parrinello–Rahman barostat with relaxation times of 2.5 and 1.0 ps, respectively. The production run was carried out for 50 ns for each model. Models for 11 different temperatures (from 240 to 440 K) and a pressure of 1 bar were generated. 5000 equally spaced snapshots of the production run were used for averaging the volumetric properties for each temperature. To control the influence of periodic boundary conditions, we made also larger models, containing 16 838 water molecules for temperatures of 260, 340, and 420 K. It was found that the characteristics studied coincide for the larger and smaller models.

Details of the Voronoi–Delaunay method have been described in our recent works,^{19,24,25} and the method has already been successfully applied to solutions of the polypeptide hIAPP²⁰ for which MD simulations are available as well.²⁶ Briefly, we first carried out the Voronoi–Delaunay tessellation for each protein configuration in solution. The molecules of the solvent (the water molecules) are considered as uniform spheres that are centered on the oxygen atom. The atoms of the protein are considered as spheres with diameters equal to the values of their Lennard-Jones parameters, σ , used in the molecular dynamics simulation. In this work we use only the radical (power) Voronoi–Delaunay tessellation²⁷ as the calculation of the empty volume inside a system of overlapping spheres was implemented only for this type of tessellation.²⁵ For the S-tessellation, which is more “physical” in describing voids between spheres of different radii, no efficient method is available for the calculation of volumetric properties. However, as we have found previously,¹⁹ both the radical and S-tessellation method yield volumes that do not differ significantly and provide the same physical results. The calculation of the Voronoi–Delaunay tessellation is a straightforward task. Here, we used our own algorithms, but programs for the calculation of radical tessellations are available also in standard geometry libraries.²⁸

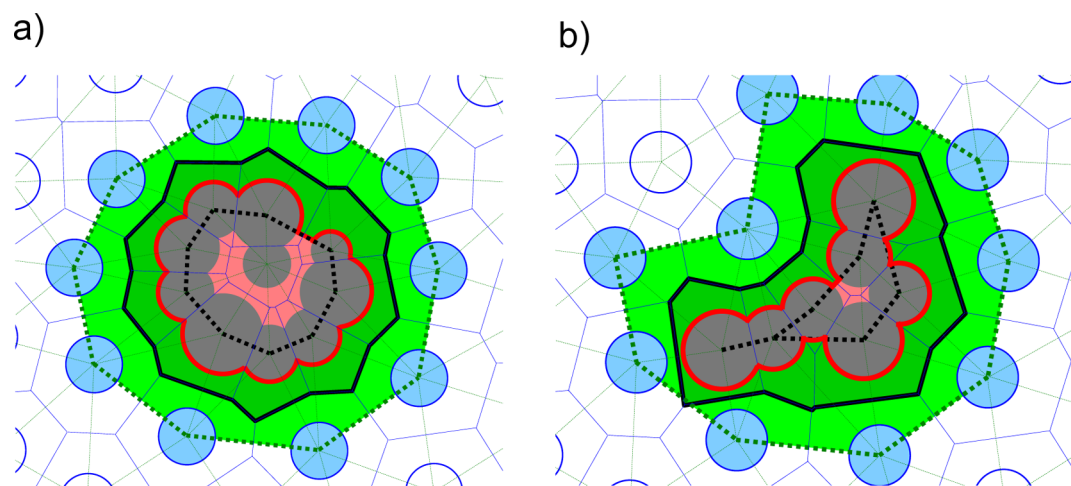


Figure 1. 2D illustration of the Voronoi–Delaunay method used for the volumetric analysis. A Voronoi cell is assigned to each particular atom and represents the volume, which is closest to it. A Delaunay simplex represents the void space between mutually neighboring atoms. Gray disks present the solute molecule. Blue and empty disks represent water molecules. Voronoi cells are shown by thin solid lines and Delaunay simplices by thin dashed lines. The Voronoi volume of the molecule, V_{Vor}^M is bounded by a thick black line. The molecular volume, V_M is bounded by thick red lines. Internal voids of the molecule, V_M^{empty} , are colored in pink. The boundary empty volume, V_B , is shown by green color: dark green is the part assigned to the molecule (V_B^M); light green is the part belonging to the solvent (V_B^S). Thick dotted lines show the boundary of the (first) Delaunay shell. Part (a) illustrates folded and part (b) unfolded polypeptides.

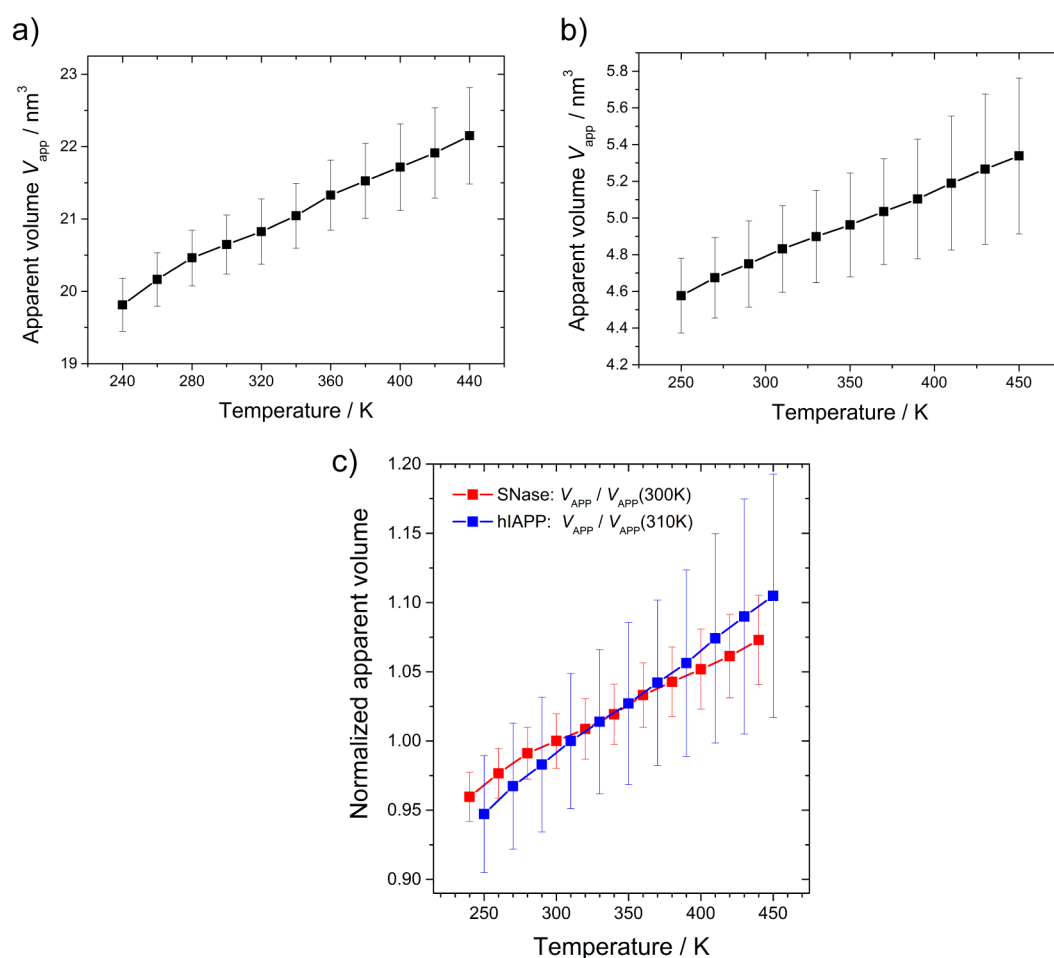


Figure 2. Temperature dependence of the apparent volume, V_{app} , of SNase (a) and hIAPP (b) and their relative temperature dependence (c) by normalization to the value at 300 K for SNase and 310 K for hIAPP, respectively (1 nm^3 corresponds to $\sim 602 \text{ mL mol}^{-1}$).

Having carried out the Voronoi–Delaunay tessellation of the solution, we decompose it into Voronoi and Delaunay shells of

the protein surface. First, one has to define the boundary Voronoi shell of the solute molecule. It consists of the Voronoi

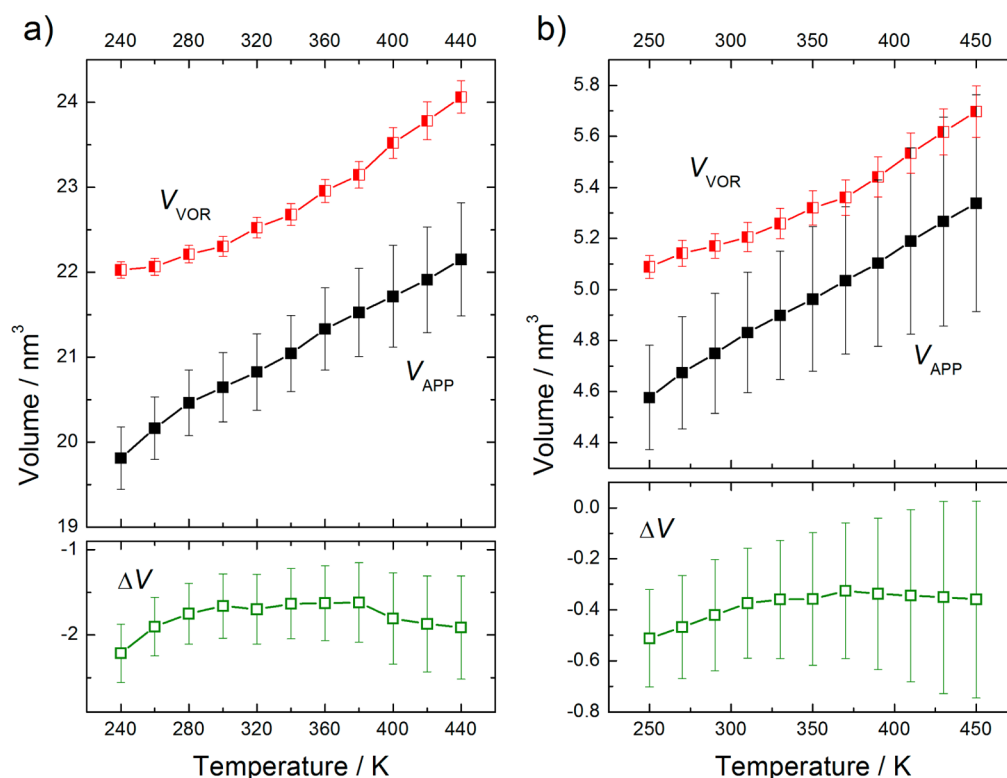


Figure 3. Decomposition of the apparent volume, V_{app} into the volume assigned to the solute molecule (Voronoi volume, V_{Vor}) and the contribution of the solvent, ΔV , for SNase (a) and hIAPP (b).

cells of the protein atoms that are adjacent to at least one atom of the solvent (water molecule), thereby establishing the set of the solvent atoms that are in contact with the solute. The former set represents the boundary shell of the solute, and the latter defines the nearest solvation shell. With this information in hand one can calculate all subsequent Voronoi shells, both going outside (to the solvent) and inside the solute molecule (if it is large enough). Thus, the Voronoi volume of a protein (the sum of the Voronoi cells of all atoms) can also be presented as the sum of the boundary and the inner Voronoi shells.

The decomposition of a solution into Voronoi shells is mathematically well-defined and can be used for determining Delaunay shells. A Delaunay shell is defined by the set of Delaunay simplexes, which have vertices (atoms) belonging to neighboring Voronoi shells. Figure 1 (dotted lines) illustrates the boundary Delaunay shell. This geometrical construction is very helpful because it can be used for the selection of boundary voids (empty space between protein and solvent: green area in Figure 1).

Calculation of the empty (or occupied) volume of a Voronoi cell of a Delaunay simplex in an ensemble of overlapping spheres is not a trivial task. A protein molecule is a typical example of such a system. An efficient solution of this problem can be found with the help of a special geometrical construction, the Voronoi–Delaunay subsimplex (simply speaking, this is the intersection of a Voronoi cell with an incident Delaunay simplex). Using this approach, we can determine the empty volume of entire Voronoi and Delaunay shells and their intersections (see ref 25 for details).

RESULTS AND DISCUSSION

Apparent Volume of the Solute. The first task of the volumetric analysis is the calculation of the partial molar

volume of the solute. In the case of our study of a protein in water, the model contains one solute molecule surrounded by water molecules. Thus, our partial molar volume is actually the apparent volume of the protein in the solvent. By definition, it can be calculated as the difference between the volume of a model box with the solution and the volume of the model box with the same amount of the pure solvent:

$$V_{app} = V_{box}^{solution} - V_{box}^{solvent} \quad (3)$$

This *direct* method requires the additional calculation of the pure solvent at the same temperature and pressure conditions.

Traditionally, it is assumed that biomolecules do not perturb the water structure at large distances. Hence, one can determine the asymptotic value of

$$V_{app}(R) = V(R) - N(R)/\rho_0 \quad (4)$$

where $V(R)$ is a volume including both the solute and its hydration shell. The parameter R characterizes the size of this region. $N(R)$ is the number of the solvent molecules, whose centers are inside the selected volume, and ρ_0 is the number density of pure water. In the case of a spherical solute, eq 4 presents the well-known Kirkwood–Buff formula for the partial molar volume,^{29–32} which can be easily applied. However, if one deals with a flexible macromolecule, this is not a simple task. In particular, one has to determine the volume inside a complex surface which is changing, following the protein's conformational dynamics. Recently, we proposed to calculate $V(R)$ as the sum of the Voronoi cell volumes of all atoms with centers inside the defined R -surface. This method turned out to be very efficient, and we coined it the *combined method* in our work.^{19,33,34}

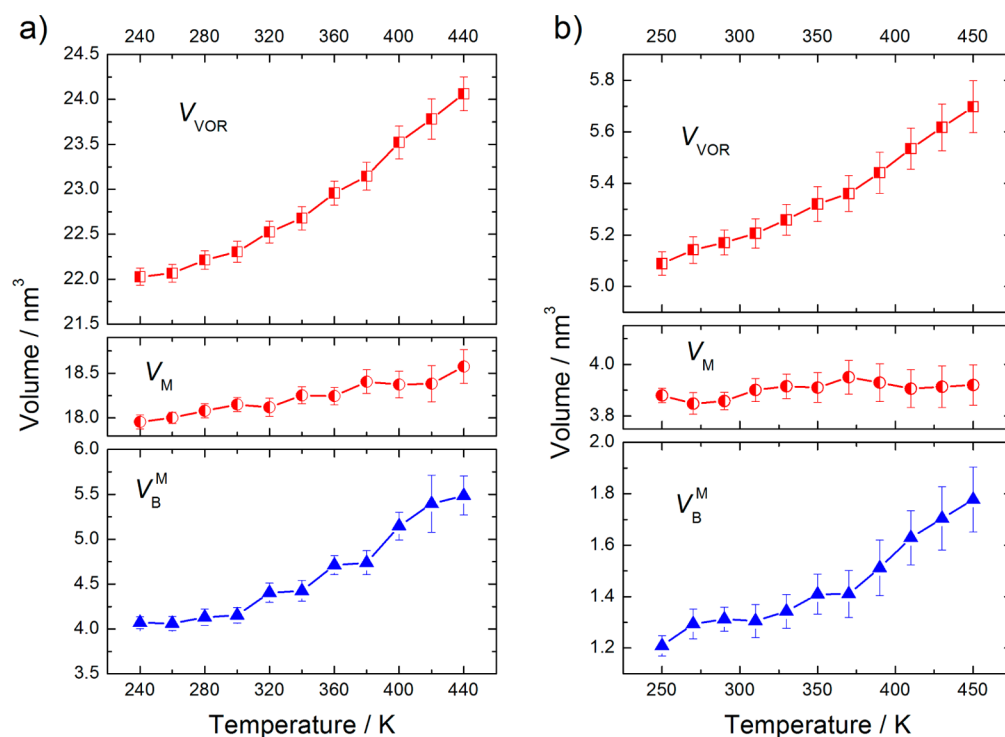


Figure 4. Temperature dependence of the Voronoi volume of the solute molecule, V_{VOR} , and its components, the molecular volume, V_M , and the part of boundary empty space, V_B^M , for SNase (a) and hIAPP (b).

In Figure 2 we show the apparent volumes, V_{app} , for SNase and, for comparison, of hIAPP, calculated with the help of eq 4 for different temperatures. Vertical lines illustrate the mean-square fluctuations of the values calculated from the MD snapshots, which amount to “error bars” of about 2.5% for SNase and 6% for hIAPP. As we will see below, these variations are mainly affected by fluctuations of the surrounding water. For both molecules, V_{app} increases practically linearly in the whole temperature interval covered, and the overall relative change, $V_{app}(T)/V_{app}(\sim 300\text{ K})$, is rather similar for both polypeptides, as demonstrated in Figure 2c. SNase being a typical folded and hIAPP a largely unfolded polypeptide, this similarity suggests that the temperature dependence of V_{app} is essentially independent of the specific chemical makeup of the polypeptide, but rather determined by the universal influence of the solvating water molecules; i.e., the surrounding interfacial water seems to contribute mainly to the temperature dependence of V_{app} . There are some small differences, however. The expansion of the folded SNase is slightly smaller than that of IAPP. This is similar to the observation that the volume of folded proteins is larger than that of unfolded proteins at low temperature, but because the expansivity is higher, the volume of the unfolded protein is larger than that of the folded protein at high temperatures. This explains the large decrease in magnitude and even change of sign in the volume change of unfolding, $\Delta V_u = V_{app}^{unf} - V_{app}^{native}$, that has been observed upon increasing temperature.¹⁴

Disentangling the Various Components of the Apparent Volume. The simplest decomposition of the apparent volume of the solute divides V_{app} into the *intrinsic volume*, V_{int} , and the contribution of the solvent, ΔV , as suggested in eq 2. The intrinsic volume of the solute is assigned here to the *Voronoi volume* of the solute molecule in solution, V_{VOR} . By definition, it contains all points of space that are closer

to the atoms of the given molecule than to any atoms of the solvent. Thus, the simplest representation of the apparent volume in our approach is

$$V_{app} = V_{VOR} + \Delta V \quad (5)$$

The calculation of V_{VOR} is readily performed having a computer model of the solute in solution. With the knowledge of V_{app} , we can then determine the solvent contribution $\Delta V = V_{app} - V_{VOR}$. Figure 3 shows the temperature dependence of V_{app} in comparison to that of its components V_{VOR} and ΔV . The data show that the hydration contribution of the solvent, ΔV , for SNase is also negative, as it was for found for hIAPP. In other words, the density of water around the Voronoi region of both polypeptides is higher than in the bulk. Fluctuations in the ΔV values are larger than those of V_{VOR} . Note that V_{VOR} increases strongly with temperature, whereas ΔV is much less temperature dependent.

The Voronoi volume, V_{VOR} , of the solute molecules can now be dissected into the *molecular volume*, V_M , and the part of boundary empty space, V_B^M , that is attributed to the solute (dark green area in Figure 1 for an illustration):

$$V_{VOR} = V_M + V_B^M \quad (6)$$

In turn, the molecular volume can be written as

$$V_M = V_M^{vdW} + V_M^{empty} \quad (7)$$

where V_M^{vdW} is the van der Waals volume (the volume of the entirety of all atoms of the solute molecule) and V_M^{empty} is the volume of internal voids. Figures 4 and 5 show the temperature dependence of these volumetric parameters. As we can see, the molecular volume V_M presents the main part of the Voronoi volume of the solute (Figure 4). However, the main change of V_{VOR} of SNase with temperature is due to the voids at the solute/solvent interface (“boundary voids”), V_B^M , contributing

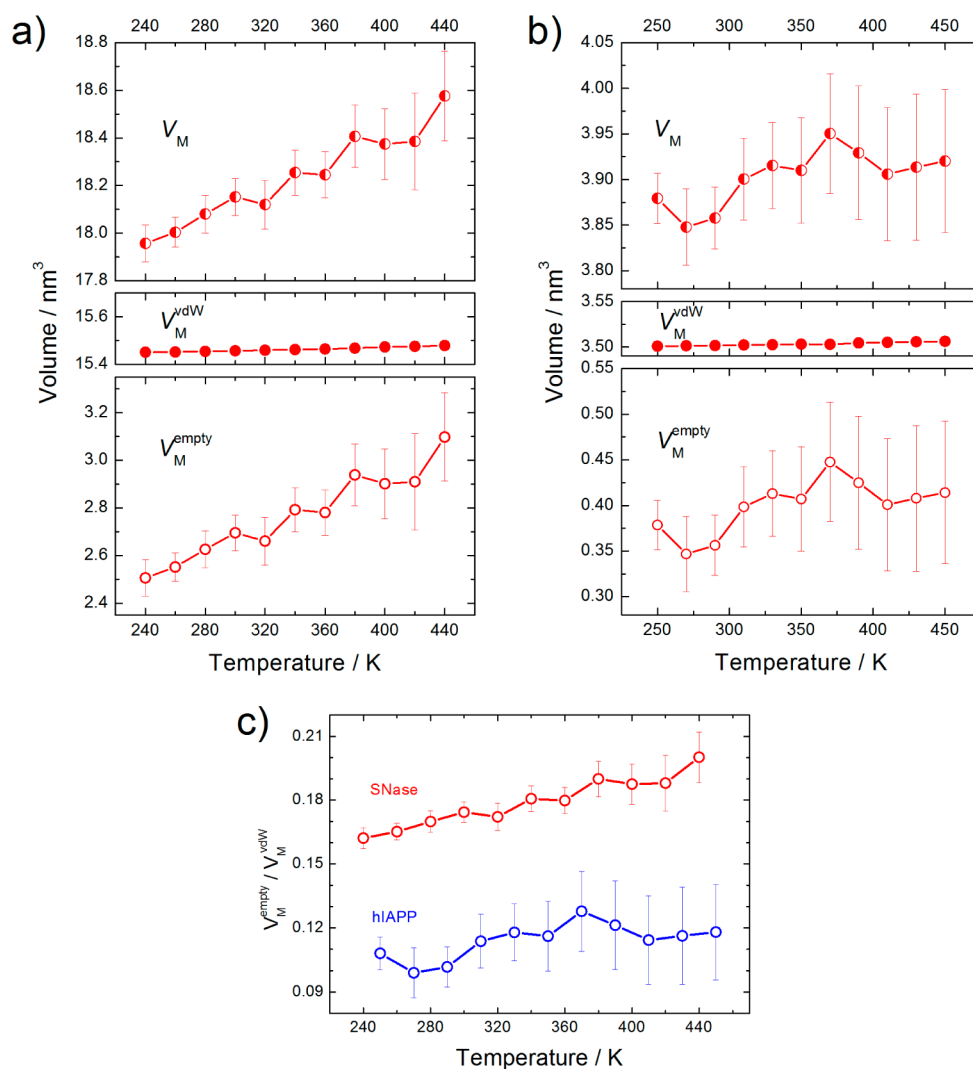


Figure 5. Components of the molecular volume, V_M , of the polypeptides (van der Waals volume of the solute molecule, V_M^{vdW} , and the empty volume inside the solute molecule, V_M^{empty}). SNase (a) and hIAPP (b) and the ratio of the components V_M^{empty} and V_M^{vdW} for both polypeptides (c).

an increase of 1.5 nm³ in comparison to 0.5 nm³ for V_M in the whole temperature interval studied (Figure 4a). For hIAPP, the situation is slightly different: We do not see a systematic increase of V_M with temperature in this case, and V_B^M determines all changes of V_{Vor} with temperature (Figure 4b).

The temperature dependence of the molecular volume, V_M , of SNase is essentially the result of the internal voids, i.e., of $V_M^{empty}(T)$, and, as expected, the van der Waals volume is practically temperature independent for both proteins (Figure 5). At the same time, the van der Waals volume, V_M^{vdW} , represents the main part of the volume of the polypeptide hIAPP. The internal voids, V_M^{empty} , make up 14–17% of the molecular volume, V_M , of SNase and 9–11% of that of hIAPP. The ratio V_M^{empty}/V_M^{vdW} as a function of temperature is depicted in Figure 5c.

Note that in our Voronoi–Delaunay approach V_M^{empty} is the entire empty volume of the solute molecule; i.e., it includes large cavities as well as narrow gaps. A largely unfolded polypeptide such as hIAPP can contain such “internal” void volume as well (see illustration in Figure 1b). Obviously, in this case, this contribution is essentially the result of conformational fluctuations of the molecule, which have in fact been observed in MD simulations.²⁶ Thus, it is not surprising that the

fluctuations of V_M^{empty}/V_M^{vdW} for hIAPP are much larger than those for SNase (Figure 5c). The fraction of these internal voids relative to the exposed surface area is much smaller for the IAPP compared to SNase, however.

Boundary Volume between Solute and Solvent. Of particular interest is the contribution of voids between the solute and solvent to the volumetric properties of the solute and its components. Geometrically, it can be extracted with the help of Delaunay simplexes.^{24,25} The dotted lines in Figure 1 illustrate the borders of the “first Delaunay shell”, which covers the boundary region between the solute molecule and solvent. The empty volume of this shell (we denote it V_B) is shown by green (light and dark). The Voronoi surface divides V_B into two parts: the internal part assigned to the solute, V_B^M , and the outer part, V_B^S , belonging to the solvent. Please note that the volume V_B is not a component of the apparent volume because its parts are accounted for in V_{app} in a different manner. V_B^M is part of the intrinsic (Voronoi) volume, V_{Vor} , and consequently is an explicit part of the apparent volume. But the solvent contribution V_B^S is not; it has to be accounted for with respect to the voids in bulk water (for details see ref 20). Nevertheless, it is interesting to see the behavior of these two boundary regions as a function of temperature, which are depicted in

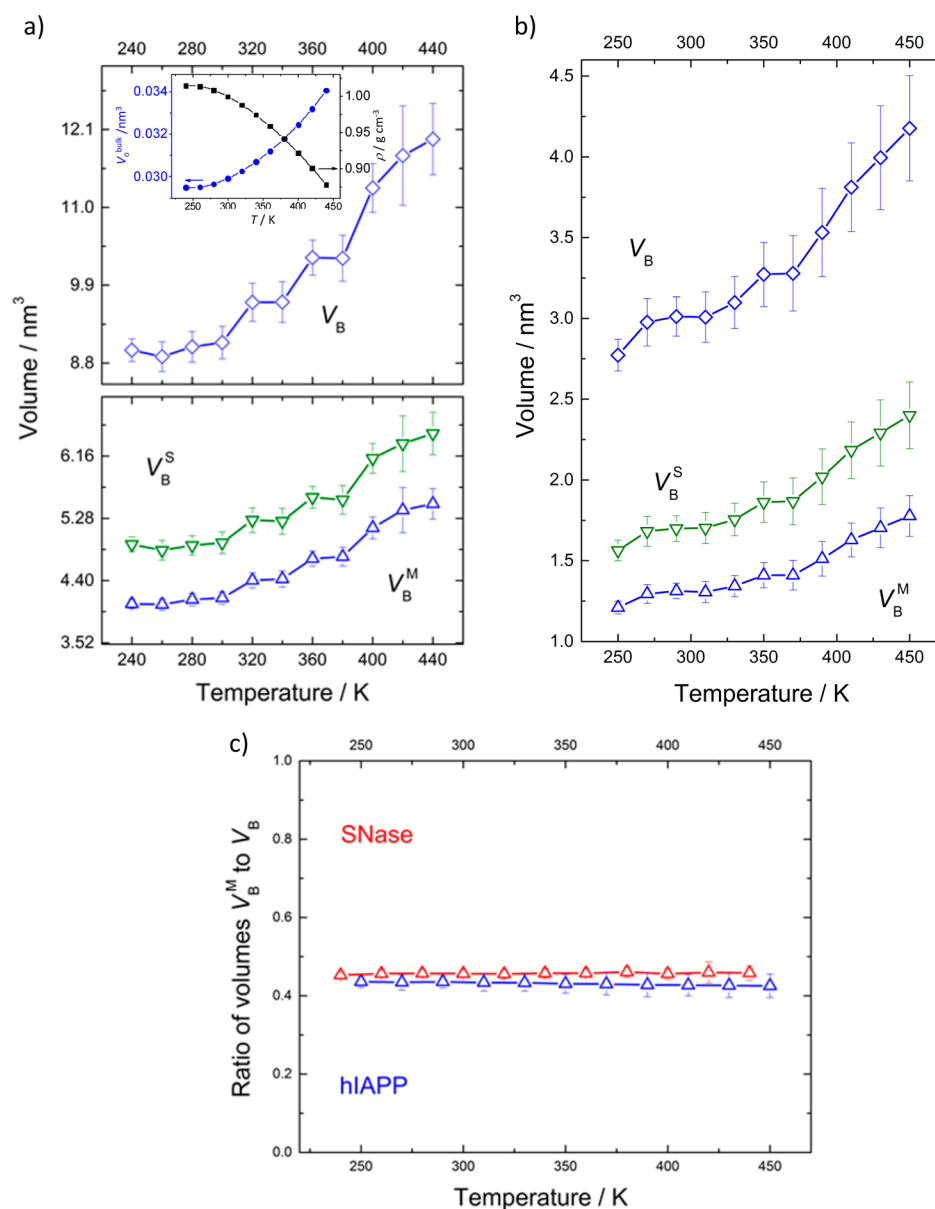


Figure 6. Boundary empty volume, V_B , and its components V_B^M and V_B^S as a function of temperature for SNase (a), hIAPP (b), and the ratio V_B^M/V_B of both peptides (c). The inset in (a) shows the temperature dependence of the density of SPC/E water used as solvent. Black squares show the density in g cm^{-3} (right axis), and blue circles show the mean volume of Voronoi cells of water molecules outside of 8 Å from the solute (left axis).

Figure 6. First, we note that the boundary volume, V_B , increases strongly with temperature. The overall change of V_B is $\sim 30\%$ in the temperature interval studied. This value is twice as large as the increase of the volume of bulk water ($\sim 15\%$) calculated as Voronoi volume of the bulk water molecules (see inset in Figure 6a, left axis). A slightly stronger growth of the boundary voids with temperature was observed for hIAPP (Figure 6b).²⁰ Thus, we confirm our previous conclusion that the boundary voids increase with temperature faster than the voids in the bulk solvent.²⁰

The values of $V_B^M(T)$ and $V_B^S(T)$ behave similarly for both peptides, indicating that they are geometrical parts of one physical characteristics, $V_B(T)$. Note that the fraction of V_B^M contributing to V_B , i.e. V_B^M/V_B , is very close for SNase and hIAPP (Figure 6c). Hence, we may presume that the boundary region is the main and universal reason for the thermal expansion of the apparent volume of polypeptides.

Temperature Dependence of the Coefficients of Thermal Expansion.

We finally discuss the temperature derivatives of the volumetric parameters, i.e., the thermal expansivity values for V_{app} , and its contributions from V_M , V_B^M , and ΔV . Owing to the fluctuations, calculation of the coefficients of thermal expansion $\alpha(T)$ is less accurate. Therefore, we approximate our $V(T)$ data by linear functions (Figure 7) to facilitate estimation of the contributions to $\alpha(T)$ more precisely (collected in Table 1).

Interestingly, some of the $V(T)$ data, in particular $V_B^M(T)$ and $\Delta V(T)$, seem to exhibit a break of the slope at about 340 K; i.e., the expansivity data below 340 K and above 340 K differ significantly (Table 1). For SNase, α_B^M increases from 1.98×10^{-4} to $4.31 \times 10^{-4} \text{ K}^{-1}$, and the hydration contribution $\Delta\alpha$ decreases from 3.07×10^{-4} to $-1.01 \times 10^{-4} \text{ K}^{-1}$ at higher temperatures. On the other hand, the coefficient of thermal expansion of V_{app} , α_{app} , is—within the experimental error—

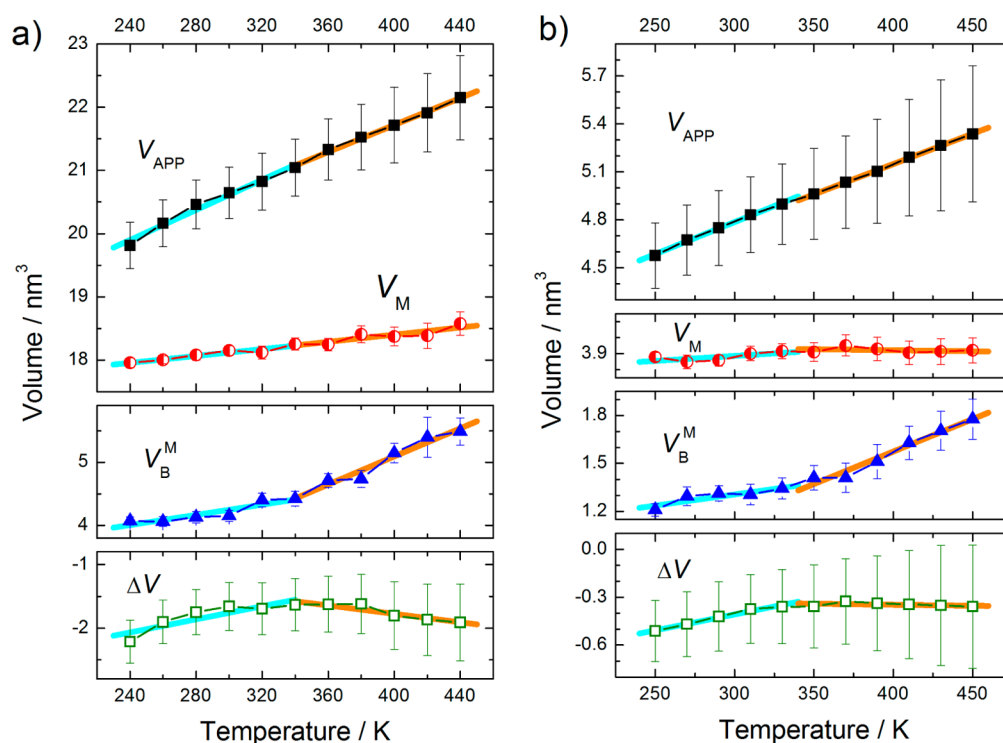


Figure 7. Estimation of the coefficient of thermal expansion, $\alpha(T)$, for the apparent volume and its components of SNase (a) and hIAPP (b). The curves are approximated by linear functions.

Table 1. Coefficients of Thermal Expansion, $\alpha = (dV/dT)/V$, for V_{app} and Its Components of SNase and hIAPP^a

$\alpha = (dV/dT)/V$	α/K^{-1} of SNase			α/K^{-1} of hIAPP		
	all T	$T \leq 340$ K	$T \geq 340$ K	all T	$T \leq 340$ K	$T \geq 340$ K
$(dV_{\text{app}}/dT)/V_{\text{app}}$	5.72×10^{-4}	6.33×10^{-4}	5.16×10^{-4}	7.79×10^{-4}	8.51×10^{-4}	7.19×10^{-4}
$(dV_M/dT)/V_{\text{app}}$	1.58×10^{-4}	1.29×10^{-4}	1.86×10^{-4}	0.25×10^{-4}	0.33×10^{-4}	-0.18×10^{-4}
$(dV_B^M/dT)/V_{\text{app}}$	3.10×10^{-4}	1.98×10^{-4}	4.31×10^{-4}	5.88×10^{-4}	4.46×10^{-4}	7.05×10^{-4}
$(d\Delta V/dT)/V_{\text{app}}$	1.04×10^{-4}	3.07×10^{-4}	-1.01×10^{-4}	1.67×10^{-4}	3.72×10^{-4}	-0.05×10^{-4}

^aThe values of α are estimated using straight line approximations: for the overall temperature region covered (columns all T), for the region below 340 K (columns $T \leq 340$ K), and for the temperature region above 340 K (columns $T \geq 340$ K).

essentially linear over the whole temperature range, adopting values of about 6.3×10^{-4} to $5.16 \times 10^{-4} \text{ K}^{-1}$ (or $5.72 \times 10^{-4} \text{ K}^{-1}$ calculated for the overall temperature region) for SNase. The corresponding experimental value obtained by pressure perturbation calorimetry (PPC) in the folded state of SNase amounts to about 7.5×10^{-4} to $6.0 \times 10^{-4} \text{ K}^{-1}$ in the temperature range between 281 and 323 K.¹⁷ These values are in good agreement with the simulation data in that temperature range.

The experimental unfolding temperature of SNase is $T_m = 333$ K, which is close to the discussed inflection point. However, we are not inclined to suggest that the change in slope of the V_B^M and ΔV curves at 340 K is a result of the unfolding of SNase. We rather believe it is a result of the nonlinear change of the boundary voids (V_B , Figure 6a) and the bulk water density (insert in Figure 6a) with temperature.

On the other hand, the apparent volume increases practically linearly with temperature. This is because the temperature-dependent changes of V_B^M and ΔV compensate each other to a large extent. Indeed, from eqs 5 and 6 we see that

$$V_{\text{app}} = V_M + V_B^M + \Delta V \quad (8)$$

There is an alternative decomposition of V_{app} , which uses the whole boundary voids, V_B , thereby omitting the term ΔV :²⁰

$$V_{\text{app}} = V_M + V_B - V_B^{S,\text{bulk}} \quad (9)$$

where the volume term $V_B^{S,\text{bulk}}$ behaves with temperature as bulk water. Thus, we can conclude that the thermal expansion of the apparent volume of a solute, V_{app} , depends on the thermal expansion of its internal voids, the boundary voids, and bulk water.

CONCLUSIONS

We used the decomposition of the molecular dynamics models of a typical folded monomeric protein, SNase, into Voronoi and Delaunay shells to study and analyze the temperature behavior of the apparent volume of the protein, V_{app} , and its contributing components in aqueous solution: the intrinsic (Voronoi) volume of the solute molecule, V_{Vor} , the molecular volume, V_M , which consists of the van der Waals volume, V_M^{vdW} , and its internal empty space, V_M^{empty} , and the contribution of the solvent, ΔV . Additionally, we geometrically separated the boundary volume V_B at the solute/solvent interface into two parts, which are assigned to the macromolecule, V_B^M , and the solvent, V_B^S .

The calculated coefficient of thermal expansion of V_{app} , α_{app} , is—within the experimental error—grossly constant over the whole temperature range covered and is in good agreement with the experimental value obtained by pressure perturbation calorimetry (PPC) in the folded state of SNase in the temperature range between 281 and 323 K.¹⁷

We show that the strong increase of V_{app} with temperature is essentially due to the expansion of the surrounding boundary layer, V_{B} . In other words, the volume in the boundary region expands with temperature more than the bulk solvent. In agreement with the “thermal volume” picture put forward by Chalikian,¹⁵ the void volume, created in the boundary region between solute and solvent, determines the temperature dependence of V_{app} to a major extent. The fact that polypeptides of different chemical nature—SNase being a typical folded protein with an essentially hydrophilic solvent accessible surface area and hIAPP a rather hydrophobic natively unfolded polypeptide—feature a very similar temperature dependence suggests that the temperature behavior of V_{app} is universal and largely independent of the chemical nature of the polypeptide; i.e., the boundary/hydration part seems to contribute mainly to the temperature dependence of V_{app} .

The less pronounced but still significant part of the temperature dependence of the apparent volume is produced by the molecular volume of the solute, V_{M} . It is the result of the expansivity of its internal voids, i.e. of $V_{\text{M}}^{\text{empty}}$, as the van der Waals contribution, $V_{\text{M}}^{\text{vdW}}$, is practically independent of temperature. As expected, the temperature dependence of $V_{\text{M}}^{\text{empty}}$ is more pronounced for the folded native protein, SNase, which has more internal voids and packing defects. The internal voids contribute about 10–20% to the molecular volume, V_{M} . Owing to the conformational dynamics of the largely unfolded hIAPP, which transiently acquires secondary structure elements only,²⁶ fluctuations of $V_{\text{M}}^{\text{empty}}$ are more pronounced compared to those of the compact structure of SNase.

While the voids in the boundary region are clearly the main contributing factor to the expansion of both the folded and unfolded polypeptides, the difference between the two comes from expansion of inner voids in the folded peptide. This expansion is relatively small for SNase because of the constraints against expansion afforded by the internal interactions of the folded chain. And the exposed surface area is smaller for the folded protein (with respect to total volume or size), so overall the expansion of the folded protein can be smaller than that of the unfolded one (the fraction of internal voids relative to the exposed surface area is much smaller for the IAPP), as seen in Figure 2. This also explains the strong temperature dependence of the volume change of unfolding of proteins such as SNase.¹⁴

The hydration contribution ΔV as defined by eq 5 is negative for both polypeptides and little temperature dependent. Its behavior results from the competition between the thermal expansion of the boundary voids and bulk water. The impact of the solute on the local density of the solvent is short ranged and limited to the first Voronoi shell around the solute.

To conclude, we hope that our results are able to shine new light on the long debate surrounding the physical basis for understanding and decomposing the volumetric properties of proteins and biomolecules in general. Our results show directly that the volumetric properties of proteins are strongly coupled to changes of the hydrational properties at the interface with

respect to the bulk properties of the solvent as well as to the expansivity of the internal voids of the protein.

The Voronoi–Delaunay tessellation approach presented here for resolving volumetric properties into their internal molecular, interfacial, and hydrational contributions might enable us to unravel the various volumetric contributions of more complex biological problems in future studies, including protein–ligand interactions, drug targeting, ion channel conduction, and enzymatic reactions. Furthermore, the method employed here might help in better understanding and interpreting volume-related experimental data, including measurements of the coefficients of thermal expansion and compressibility of biomolecules.

AUTHOR INFORMATION

Corresponding Author

*(R.W.) E-mail roland.winter@tu-dortmund.de; Ph +49 231 755 3900.

Notes

The authors declare no competing financial interest.

ACKNOWLEDGMENTS

Financial support from Alexander von Humboldt foundation, grants from RFFI (No. 12-03-00654), and the DFG (Cluster of Excellence RESOLV (EXC 1069)) are gratefully acknowledged. We thank Dr. M. Andrews for providing us with the trajectories of his hIAPP simulations.

REFERENCES

- (1) Privalov, P. L.; Gill, S. J. Stability of Protein Structure and Hydrophobic Interaction. *Adv. Protein Chem.* **1988**, *39*, 191–234.
- (2) Dill, K. A. Dominant Forces in Protein Folding. *Biochemistry* **1990**, *29*, 7133–7155.
- (3) Levy, Y.; Onuchic, J. N. Water Mediation in Protein Folding and Molecular Recognition. *Annu. Rev. Biophys. Biomol. Struct.* **2006**, *35*, 389–415.
- (4) Brandts, J. F.; Oliveira, R. J.; Westort, C. Thermodynamics of Protein Denaturation. Effect of Pressure on the Denaturation of Ribonuclease A. *Biochemistry* **1970**, *9*, 1038–1047.
- (5) Zipp, A.; Kauzmann, W. Pressure Denaturation of Metmyoglobin. *Biochemistry* **1973**, *12*, 4217–4228.
- (6) Hawley, S. A. Reversible Pressure-Temperature Denaturation of Chymotrypsinogen. *Biochemistry* **1971**, *10*, 2436–2442.
- (7) Royer, C. A. Revisiting Volume Changes in Pressure-Induced Protein Unfolding. *Biochim. Biophys. Acta, Protein Struct. Mol. Enzymol.* **2002**, *1595*, 201–209.
- (8) Silva, J. L.; Foguel, D.; Royer, C. A. Pressure Provides New Insights into Protein Folding, Dynamics and Structure. *Trends Biochem. Sci.* **2001**, *26*, 612–618.
- (9) Heremans, K.; Smeller, L. Protein Structure and Dynamics at High Pressure. *Biochim. Biophys. Acta, Protein Struct. Mol. Enzymol.* **1998**, *1386*, 353–370.
- (10) Akasaka, K. Probing Conformational Fluctuation of Proteins by Pressure Perturbation. *Chem. Rev.* **2006**, *106*, 1814–1835.
- (11) Winter, R.; Lopes, D.; Grudzielanek, S.; Vogtt, K. Towards an Understanding of the Temperature/Pressure Configurational and Free-Energy Landscape of Biomolecules. *J. Non-Equilib. Thermodyn.* **2007**, *32*, 41–97.
- (12) Mishra, R.; Winter, R. Cold- and Pressure-Induced Dissociation of Protein Aggregates and Amyloid Fibrils. *Angew. Chem., Int. Ed.* **2008**, *47*, 6518–6521.
- (13) Suladze, S.; Kahse, M.; Erwin, N.; Tomazic, D.; Winter, R. Probing Volumetric Properties of Biomolecular Systems by Pressure Perturbation Calorimetry (PPC) - The Effects of Hydration, Cosolvents and Crowding. *Methods* **2014**, DOI: 10.1016/j.jymeth.2014.08.007.

- (14) Mitra, L.; Rouget, J. B.; Garcia-Moreno, B.; Royer, C. A.; Winter, R. Towards a Quantitative Understanding of Protein Hydration and Volumetric Properties. *ChemPhysChem* **2008**, *9*, 2715–2721.
- (15) Chalikian, T. V. Volumetric Properties of Proteins. *Annu. Rev. Biophys. Biomol. Struct.* **2003**, *32*, 207–235.
- (16) Chalikian, T. V.; Totrov, M. M.; Abagyan, R. A.; Breslauer, K. J. The Hydration of Globular Proteins as Derived from Volume and Compressibility Measurements: Cross Correlating Thermodynamic and Structural Data. *J. Mol. Biol.* **1996**, *260*, 588–603.
- (17) Mitra, L.; Smolin, N.; Ravindra, R.; Royer, C.; Winter, R. Pressure Perturbation Calorimetric Studies of the Solvation Properties and the Thermal Unfolding of Proteins in Solution: Experiments and Theoretical Interpretation. *Phys. Chem. Chem. Phys.* **2006**, *8*, 1249–1265.
- (18) Brovchenko, I.; Burri, R. R.; Krukau, A.; Oleinikova, A.; Winter, R. Intrinsic Thermal Expansivity and Hydrational Properties of Amyloid Peptide A β 42 in Liquid Water. *J. Chem. Phys.* **2008**, *129*, 195101.
- (19) Voloshin, V. P.; Medvedev, N. N.; Andrews, M. N.; Burri, R. R.; Winter, R.; Geiger, A. Volumetric Properties of Hydrated Peptides: Voronoi-Delaunay Analysis of Molecular Simulation Runs. *J. Phys. Chem. B* **2011**, *115*, 14217–14228.
- (20) Voloshin, V. P.; Kim, A. V.; Medvedev, N. N.; Winter, R.; Geiger, A. Calculation of the Volumetric Characteristics of Biomacromolecules in Solution by the Voronoi-Delaunay Technique. *Biophys. Chem.* **2014**, *192*, 1–9.
- (21) Hess, B.; Kutzner, C.; van der Spoel, D.; Lindahl, E. GROMACS 4: Algorithms for Highly Efficient, Load-Balanced, and Scalable Molecular Simulation. *J. Chem. Theory Comput.* **2008**, *4*, 435–447.
- (22) Pronk, S.; Pall, S.; Schulz, R.; Larsson, P.; Bjelkmar, P.; Apostolov, R.; Shirts, M. R.; Smith, J. C.; Kasson, P. M.; van der Spoel, D.; et al. GROMACS 4.5: A High-Throughput and Highly Parallel Open Source Molecular Simulation Toolkit. *Bioinformatics* **2013**, *29*, 845–854.
- (23) Oleinikova, A.; Smolin, N.; Brovchenko, I.; Geiger, A.; Winter, R. Formation of Spanning Water Networks on Protein Surfaces via 2D Percolation Transition. *J. Phys. Chem. B* **2005**, *109*, 1988–1998.
- (24) Kim, A. V.; Voloshin, V. P.; Medvedev, N. N.; Geiger, A. Decomposition of a Protein Solution into Voronoi Shells and Delaunay Layers: Calculation of the Volumetric Properties. In *Transactions on Computational Science XX*; Gavrilova, M. L., Tan, C. J. K., Kalantari, B., Eds.; Springer: Berlin, 2013; Vol. 8110, pp 56–71.
- (25) Voloshin, V. P.; Medvedev, N. N.; Geiger, A. Fast Calculation of the Empty Vol. in Molecular Systems by the use of Voronoi-Delaunay Subsimplexes. In *Transactions on Computational Science XXII*; Gavrilova, M. L., Ed.; Springer: Berlin, 2014; Vol. 8360, pp 156–172.
- (26) Andrews, M. N.; Winter, R. Comparing the Structural Properties of Human and Rat Islet Amyloid Polypeptide by MD Computer Simulations. *Biophys. Chem.* **2011**, *156*, 43–50.
- (27) Aurenhammer, F. Power Diagrams: Properties, Algorithms and Applications. *SIAM J. Sci. Comput.* **1987**, *16*, 78–96.
- (28) CGAL Computational Geometry Algorithms Library CGAL, <http://www.cgal.org>.
- (29) Ben-Naim, A. *Molecular Theory of Solutions*; Oxford University Press: Oxford, 2006.
- (30) Kirkwood, J. G.; Buff, F. P. The Statistical Mechanical Theory of Solutions. I. *J. Chem. Phys.* **1951**, *19*, 774–777.
- (31) Imai, T.; Kovalenko, A.; Hirata, F. Partial Molar Volume of Proteins Studied by the Three-Dimensional Reference Interaction Site Model Theory. *J. Phys. Chem. B* **2005**, *109*, 6658–6665.
- (32) Patel, N.; Dubins, D. N.; Pomes, R.; Chalikian, T. V. Parsing Partial Molar Volumes of Small Molecules: A Molecular Dynamics Study. *J. Phys. Chem. B* **2011**, *115*, 4856–4862.
- (33) Medvedev, N. N.; Voloshin, V. P.; Kim, A. V.; Anikeenko, A. V.; Geiger, A. Calculation of Partial Molar Volume and Its Components for Molecular Dynamics Models of Dilute Solutions. *J. Struct. Chem.* **2013**, *54*, 271–288.
- (34) Kim, A. V.; Medvedev, N. N.; Geiger, A. Molecular Dynamics Study of the Volumetric and Hydrophobic Properties of the Amphiphilic Molecule C8E6. *J. Mol. Liq.* **2014**, *189*, 74–80.